Proceedings of the 33rd European Safety and Reliability Conference (ESREL 2023)
Edited by Mário P. Brito, Terje Aven, Piero Baraldi, Marko Čepin and Enrico Zio
 Published by Research Publishing, Singapore.
doi: 10.3850/978-981-18-8071-1_P502-cd

Numerical modelling of liquid hydrogen tanks performance during fire engulfment

Alice Schiaroli

Department of Mechanical and Industrial Engineering, NTNU, Norway. E-mail: alicesc@ntnu.no
Department of Civil, Chemical, Environmental and Materials Engineering, University of Bologna, Italy E-mail: alice.schiaroli@unibo.it

Giordano Emrys Scarponi

Department of Civil, Chemical, Environmental and Materials Engineering, University of Bologna, Italy. E-mail: giordano.scarponi@unibo.it

Valerio Cozzani

Department of Civil, Chemical, Environmental and Materials Engineering, University of Bologna, Italy. E-mail: valerio.cozzani@unibo.it

Federico Ustolin

Department of Mechanical and Industrial Engineering, NTNU, Norway. E-mail: federico.ustolin@ntnu.no

The incumbent need to tackle global warming draws attention to potential zero-emission energy solutions. Liquid hydrogen (LH_2) is a carbon-free energy carrier, and it is then foreseen to play a vital role in the decarbonization process of the global transportation sector, which is proved to be one of the most impactful in terms of greenhouse gas (GHG) production. Despite the benefits of LH_2 (e.g., reduced storage space, high energy density), many safety concerns arise from its application. From a safety standpoint, the exposure of a cryogenic tank to an external fire is the worst-case scenario that can result into severe consequences.
In the present study, a computational fluid dynamic (CFD) analysis is carried out to investigate the behaviour of a cryogenic hydrogen storage tank in external fire conditions. The worst-case scenario when the tank is already pressurized due to the boil-off formation and the safety valve is not active due to failure is simulated by means of the developed model. The results of the analysis are compared with the outcomes of an analytical model previously developed for the same purpose and validated with available experimental data. The CFD model used in this work is able to predict the response of the vessel when the hydrogen content is in both subcritical and supercritical conditions and provides valuable information for the safety assessment of LH_2 applications.

Keywords: liquid hydrogen, hydrogen safety, external fire, CFD, supercritical, pressure build-up, time to failure

1. Introduction

Decarbonization is a recurrent theme in the global debate on the energy transition. In the attempt to reduce greenhouse gas (GHG) emissions, countries worldwide are developing new strategies to meet carbon neutrality targets by 2050. The recent growing interest in hydrogen is driven by its carbon-free nature and the resulting lack of CO_2 in the flue gas, which makes it a promising zero-emission energy carrier. Therefore, many decarbonization strategies rely on the use of hydrogen as an alternative to fossil fuels, whose combustion produces around 60% of the greenhouse gas emissions from human activities (Köne and Büke, 2010). In the next decades, the use of hydrogen is predicted to grow significantly, particularly in the transportation sector (Tarhan and Çil, 2021). To promote the fast deployment of the hydrogen-based mobility, storage and transportation issues need to be tackled. The choice of the appropriate storage solution depends on several constraints, such as the storage space available on board, the amount of fuel required to guarantee and acceptable driving range and the request of a gravimetric density (i.e., the ratio between the mass of fuel and the mass of the system fuel-tank) of 7.5 wt%, as

established by the US Department of Energy (DOE) (Hwang and Varma, 2014). The challenge is to comply with these limitations by finding an efficient storage technology able to increase the low hydrogen density sufficiently. In these terms, liquefaction is one of the most effective and feasible options (Yin and Ju, 2020). In parallel with the environmental benefits mentioned above, the introduction of hydrogen in the transportation sector poses safety as a matter of fundamental importance. Hydrogen has peculiar flammability properties (e.g., wider flammability limits, lower ignition energy) compared to conventional hydrocarbon-based fuels, like gasoline or natural gas. Thus, safety concerns about its applications are more significant (Crowl and Jo, 2007). Among the possible accident scenarios, the exposure of a liquid hydrogen (LH_2) storage tank to an external fire is the most critical and can lead to the catastrophic rupture of the tank. In the worst case, the sudden failure of the tank can result into a boiling liquid expanding vapor explosion (BLEVE), that is a physical explosion that follows the release of a large mass of pressurized superheated liquid in the atmosphere (CCPS, 1999). Furthermore, hydrogen has a very low critical pressure (12.964 bar (NIST, 2019)). Therefore, a supercritical BLEVE might be generated after the tank rupture and its yield must be considered during the consequence analysis (Ustolin et al., 2020a). Studies are required to investigate the response of the hydrogen content and estimate relevant parameters, such as the time to failure (TTF), that are fundamental to develop safety measures, codes and standards and are a useful support in the decision-making processes regarding hydrogen safety.

In the present work, a computational fluid dynamic (CFD) analysis is carried out to study the behaviour of a cryogenic hydrogen storage tank exposed to an external fire. The model developed in this study simulates the behaviour of the LH_2 tank designed by BMW (Pehr, 1996) when engulfed in a fire under the worst circumstances: pressurized tank at 4 bar and faulty safety valve. The model developed by Ustolin et al. (2022) is used in this study to simulate hydrogen in both sub- and supercritical conditions. The results are compared with the ones provided with the analytical model purposed and validated by Ustolin et al. (2021).

2. Liquid and supercritical hydrogen

Hydrogen gas (GH_2) is converted into a cryogenic liquid when cooled below 20.4 K at atmospheric pressure. In this process, the volumetric density of the fuel significantly increases up to more than 800 times (Aziz, 2021), with obvious advantages in terms of storage capacity. The main drawback of LH_2, like for other cryogenic liquids (e.g., Liquefied Natural Gas, LNG) is the evaporation of the liquid mass that leads to the formation of the so-called boil-off gas (BOG). The major contribution to the BOG generation is the heat transfer between the cold cryogenic liquid inside the tank and the warm external environment (Jeon et al., 2021), driven by the large temperature difference (around 270 K for hydrogen, considering an average external temperature of 293 K). The pressure build-up inside the tank, caused by LH_2 vaporization, is avoided through the installation of pressure relief valves (PRVs). At least two PRVs are installed on the cryogenic tank to vent the gaseous phase and prevent pressures above the maximum allowed working pressure (MAWP), which is typically not more than 8.2 bar for commercial cryogenic vessels (Rybin et al., 2015). Given those aspects, cryogenic storage tanks are designed to minimize incoming heat fluxes and then limit venting operations.

2.1. *Storage tanks*

Cryogenic liquid hydrogen is stored in double-walled super-insulated tanks. Due to the extreme storage conditions of LH_2 (i.e., cryogenic temperatures, around 20 K), special requirements have been put forward for choosing the materials for storage and transport vessels. The inner and outer walls of the tank are commonly made of austenitic stainless steel, one of the less susceptible materials to hydrogen embrittlement. Recently, the research is also focused on aluminum alloys, particularly in the space field, and composite materials for their advantage of being lightweight (Qiu et al., 2021).

The insulation is placed in the annular space between the two walls. Different techniques can be used to prevent the heating of LH_2. Common solutions are multi-layer insulation (MLI),

powders, such as perlite and microspheres. (Barron and Nellis, 2016). An MLI system is made of alternate layers of reflective shields (e.g., Mylar of Kapton with a metal coating) and low-conductivity spacers. This design allows the minimization of both radiation and conduction. Moreover, the insulation space is usually evacuated to realize a multi-layer vacuum insulation (MLVI) and reduce the heat transfer by convection. The thermal conductivity achievable with such a system is 0.037 mW m^{-1} K^{-1} (with 0.006 mm aluminum foils and 0.015 mm fiberglass papers with a density of 20 layers cm^{-1}, and a pressure of 10^{-5} torr, boundary temperatures of 300 K and 90.5 K) (Barron and Nellis, 2016). Perlite powder is obtained by crushing and expanding the volcanic rock with heat. The powder is then filled in the vacuumed annular space and performs as an excellent insulator. The average thermal conductivity for a perlite insulation with vacuum (10^{-4} torr) is 1 mW m^{-1} K^{-1} (Hebb, 2014). Finally, microspheres are spherical particles with a diameter range between 1 and 1000 μm and are commonly made of glass. They are used in a vacuum range of 10-30 mtorr and their thermal performance is better than perlite (40-100%). They are typically used for large (10,000 m^3) and mega-scale (100,000 m^3) applications to reduce the boil-off up to 50% (Fesmire et al., 2021).

2.2. *LH_2 tanks in external fire conditions*

Safety is a crucial issue in society's public acceptance of hydrogen. Like for other fuels, hydrogen safety is related to its flammable properties. Compared to hydrocarbons (e.g., natural gas, gasoline, and diesel), hydrogen has significantly wider flammability (4-75% vol in air) and detonability (18.3-59.0% vol in air) ranges and much lower ignition energy (0.017 mJ) (Ustolin et al., 2022a). Moreover, liquid hydrogen also requires further attention because of the extreme low temperatures (Aziz, 2021). As mentioned above, from a safety standpoint the worst-case scenario for a cryogenic tank is the exposure to an external fire. In addition to the possible occurrence of the BLEVE, high temperatures and radiation affect the thermal performance of the insulator. Depending on the type of insulation, it can undergo degradation or loss of vacuum, that result in a significant increase in the thermal conductivity (Fesmire, 2017). For instance, the fire test conducted by TNO in 2015 proves that perlite experiences a relevant increase in its thermal conductivity due to exposure to the external heating source (Kamperveen et al., 2016).

The thermal conductivity of the insulator influences the response of the vessel. Moreover, it is a critical input data for analytical and CFD models and has a strong influence on their outcomes (Ustolin et al., 2022b). Its estimation is a complex task and further research is required to reduce the uncertainty by which it is still affected.

2.3. *Supercritical hydrogen*

Hydrogen has a low critical temperature (33.145 K and pressure (12.964 bar) compared with conventional fuels (NIST, 2019). Hence, it is likely that the liquid lading of an LH_2 cryogenic tank reaches supercritical conditions due to undesired heat transfer from the surroundings (Ustolin et al., 2020b). In this case, if the catastrophic rupture of the vessel occurs, the resulting BLEVE is called supercritical BLEVE. Experiments on this phenomenon have been carried out by Stawczyk (2003) and Laboureur et al. (2014). They reproduced small-scale supercritical BLEVEs by heating liquid propane vessels and assessed that, when the vessel content becomes supercritical, the trend of the inner pressure slightly changes. In fact, when the fluid reaches the critical point, the inner pressure trend deviates from the saturation line and has a linear variation with temperature. Similar results have been obtained by Ustolin et al. (2021) by applying an analytical model to estimate the TTF of an LH2 storage tank with supercritical lading. Since it is not uncommon for a cryogenic hydrogen tank to contain a supercritical fluid, the capability to simulate and reproduce the behavior of supercritical hydrogen is crucial in safety studies.

3. LH_2 fire test: BMW case study

Between 2005 and 2007, BMW Group produced the Hydrogen 7, a car with a dual-fuel internal combustion engine (BMW Group, 2007). This was the first commercial vehicle with a liquid hydrogen vessel installed on board. The automobile was equipped with a storage vessel with a volume of 0.122 m^3. In addition to the MLVI insulation, two vapor cooled shields

(VCSs) were added to reduce the heat loading (Rüdiger, 1992). The Group carried out a fire test to assess the safety of this innovative hydrogen application. The features of the LH_2 tank used in the fire test are summarized in Table 1. During the test, the tank was completely engulfed in a propane fire with a mean flame temperature of 1,193 K (Pehr 1996). The heating from the fire caused the loss of vacuum in the insulation region and the opening of the PRV after about six minutes from the beginning of the test. At the opening of the PRV, the pressure inside the tank was approximately 4.6 bar. After 14 minutes from the test start, the entire liquid phase was evaporated, and the tank content was completely vented. The results of this test are unique since few experimental data available for fire tests involving liquid hydrogen tanks exist. Despite the good quality of the outcomes, some relevant information is missing or uncertain. First, the composition of the MLVI is unknown and then its properties can only be assumed. Secondly, the diameter of the PRV is not given, not allowing to precisely calculate the venting time. Finally, values obtained from the thermocouples are graphically reported in a single chart even if they have a very wide range (1,400 K); this makes the extrapolation of data particularly difficult.

Table 1. Features of the LH_2 tank used for the BMW fire test.

Parameter	Value
Volume	0.122 m^3
Initial filling degree	55%
Initial pressure	1.06 bar
Type of insulation	MLVI
Number of layers	80
Insulation thickness	35 mm
Orientation	Horizontal

4. Methodology

In this study, a CFD analysis is carried out to study the behaviour of the lading of a hydrogen cryogenic storage tank exposed to an external fire. The 2D CFD model developed by Ustolin et al. (2022) in Ansys Fluent is used to simulate the fluid behaviour in both sub- and supercritical conditions. The LH_2 storage tank, whose feature are described in Table 1, was modelled. The mechanical response of the tank is expressed in terms of TTF. It is conservatively estimated assuming that the failure of the tank occurs when the mechanical stress reaches the admissible strength of the wall material. Since in Rüdiger (1992) the type of aluminum alloy that compose the inner tank walls is not specified, the mechanical stress of the inner wall is calculated considering the mechanical properties of 5083 Al alloy. The material admissible strength (112.5 MPa) is calculated as 90% of its yield strength (125 MPa) and the mechanical stress of the shell material is estimated using the Von-Mises criterion.

The cross-section of the tank is represented in Figure 1. Given the symmetry of the geometry, the computational domain is selected as half of the cross-section of the vessel to reduce the computational time. The mesh consists of quadrilateral and triangular elements (unstructured mesh) with a maximum size of 3 mm. Inflation layers are added in the fluid zone (both in the liquid and in the vapor space) in the proximity of the inner vessel to have a good modelling of the near wall region. In total, 25 inflation layers with a growing rate of 1.2 are present. The total number of cells is 17,029. A grid independence analysis was carried out even though not reported in this study due to space limitation. The opening of the PRV is neglected in the present analysis. The simulation time is chosen equal to 900 s (15 minutes), that is the time after the fire ignition at which the sensor of the liquid level gave the minimum value.

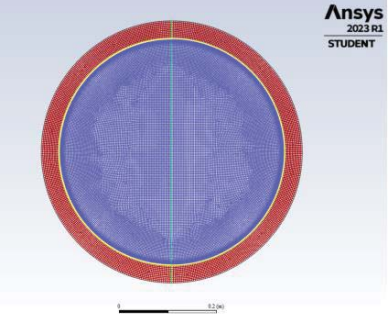

Figure 1: Cross-section of the storage tank object of the present study.

4.1. *Numerical setup*

The volume of fluid (VOF) model is selected to reproduce the multiphase features of the tank lading. For the evaporation-condensation mechanism, the Lee model is used, with the model constants equal to 0.1 s^{-1}, as by default. The k-ω shear stress transport (SST) model is used as turbulence model. For the pressure-velocity coupling the SIMPLEC (Semi-Implicit Method for Pressure Linked Equations-Consistent) method is selected, and the skewness correction is set to 0. The discretization schemes and the under-relaxation factors are the same used by Ustolin et al. (2022). The first-order implicit scheme with a time step of 0.01 s is used for the transient simulation. The set of governing equations used for the setup are summarized in Table 2.

Table 2: Equations for turbulent, two-phases and transient setup for the CFD simulation.

Parameter	Value
Energy (fluid domain)	$\frac{\partial(\rho E)}{\partial t} + \nabla \cdot [\boldsymbol{u}\,(\rho E + p)] = \nabla \cdot \left(k_{eff} \nabla T\right) + \lambda(m_{V\to L} - m_{L\to V})$ t: time; ρ: two-phase volume fraction averaged density; E: two-phase ensembled averaged specific energy; $\boldsymbol{u}$: ensembled averaged velocity; p: ensembled averaged pressure; k_{eff}: effective thermal conductivity; T: temperature; λ: latent heat of vaporization; $m_{V\to L}$: condensation liquid phase source term; $m_{L\to V}$: evaporation liquid phase source term
Energy (solid domain)	$\frac{\partial(\rho_s Cp_s T_s)}{\partial t} = \nabla \cdot (k_s \nabla T_s)$ ρ_s: solid density; Cp_s: solid heat capacity; T_s: solid temperature
Effective thermal conductivity	$k_{eff} = k + \frac{Cp\mu_T}{Pr_T}$ k: two-phase volume fraction averaged thermal conductivity; Cp: two-phase volume fraction averaged heat capacity; μ_T: two-phase volume fraction averaged turbulent viscosity; Pr_T: turbulent Prandtl number
Momentum	$\frac{\partial(\rho \boldsymbol{u})}{\partial t} + \nabla \cdot (\rho \boldsymbol{u}\boldsymbol{u}) = -\nabla \boldsymbol{p} + \rho \boldsymbol{g} + \nabla \cdot \left[\mu \left(\nabla \boldsymbol{u} + (\nabla \boldsymbol{u})^T - \frac{2}{3}\nabla \cdot \boldsymbol{u} I\right)\right] - \nabla \cdot (\rho \boldsymbol{u}' \boldsymbol{u}')$ $\boldsymbol{g}$: gravity acceleration; μ: two-phase averaged viscosity; I: identity tensor; $\boldsymbol{u}'$: instantaneous velocity fluctuation
Vapour volume fraction	$\alpha_V = 1 - \alpha_L$ α_V : vapor volume fraction ; α_L : liquid volume fraction
Liquid volume fraction	$\frac{1}{\rho_L}\left[\frac{\partial(\alpha_L \rho_L)}{\partial t} + \nabla \cdot (\alpha_L \rho_L \boldsymbol{u})\right] = m_{V\to L} - m_{L\to V}$ ρ_L : liquid density
Turbulent specific dissipation rate	$\frac{\partial(\rho\omega)}{\partial t} + \nabla \cdot (\rho\omega \boldsymbol{u}) = \nabla \cdot \left[\left(\mu + \frac{\mu_T}{\sigma_\omega}\right)\nabla\omega\right] + G_\omega - Y_\omega$ ω : turbulent specific dissipation rate; σ_ω : turbulent Prandtl number for ω ; G_ω : generative term for ω ; Y_ω : dissipative term for ω
Turbulent viscosity	$\frac{\partial(\rho K)}{\partial t} + \nabla \cdot (\rho K \boldsymbol{u}) = \nabla \cdot \left[\left(\mu + \frac{\mu_T}{\sigma_K}\right)\nabla\omega\right] + G_K - Y_K$ K : turbulent kinetic energy; σ_K : turbulent Prandtl number for ω ; G_K : generative term for K due to mean velocity gradients; Y_K : dissipative term for K due to turbulence
Two-phase averaged material properties	$\psi = \alpha_L \psi_L + (1 - \alpha_L)\psi_V$ ψ: two-phase volume fraction averaged property; ψ_L: liquid property; ψ_V: vapour property

4.2. *Boundary and initial conditions*

At the beginning of the simulation, it is supposed that the tank is already pressurized. In order to model the worst-case scenario, the initial pressure is set closer to the inner pressure that caused of opening of the PRV (4.6 bar) during the experimental test; furthermore, saturated conditions and equilibrium between the liquid and the gaseous phases have been assumed. Then, initial temperature and pressure are 4 bar and 26.076 K, respectively. The initial filling degree is 55%. The symmetry condition is imposed in the transversal axis (green line in Figure 1) of the vessel section. On the outer wall, an external radiation temperature of 1,193 K is set to reproduce the presence of the propane fire. The emissivity of the material is chosen equal to 1 to make the most conservative assumption.

4.3. *Properties*

Hydrogen properties (specific heat, density, thermal conductivity, and viscosity) are implemented as piecewise functions of the temperature (data are from NIST (2019)). The density of the vapour phase is calculated according to the Peng-Robinson equation of state. For the MLI insulation, a density of 167 kg m^{-3} and a specific heat of 881.5 J kg^{-1} K^{-1} are assumed. A user-defined function (UDF) is used to define the thermal conductivity. The initial thermal conductivity of 1.5 mW m^{-1} K^{-1} (perfectly working insulation) (Ustolin et al., 2021) is increased up to 160 mW m^{-1} K^{-1} (partially damaged insulation) after 115 s. The time is chosen based on the sudden increase in the inner pressure registered during the BMW fire test.

5. Results

The evolution of the inner pressure over time obtained with the CFD model used in the present study is shown in Figure 2. The comparison with the data from the BMW fire test is not possible because of the different initial conditions selected for the simulation and the presence of a functioning PRV during the experiments. However, the model was already validated by reproducing the fire test until the opening of the PRV (360 s) with an initial pressure of 1.06 bar (Ustolin et al., 2022b). As already mentioned in Section 2.3, it is likely that hydrogen becomes supercritical when the tank is exposed to a heat source (e.g., and external fire). The results of the CFD model indicates (see Figure 2) that the critical pressure (12.964 bar) is reached after 504 s from the beginning of the simulation. In the BMW fire test this is prevented through the action of the PRV. The outcomes of the CFD analysis can be compared with the result obtained by the analytical model developed by Ustolin et al. (2021) that was used to reproduce the BMW fire test assuming the failure of the PRV.

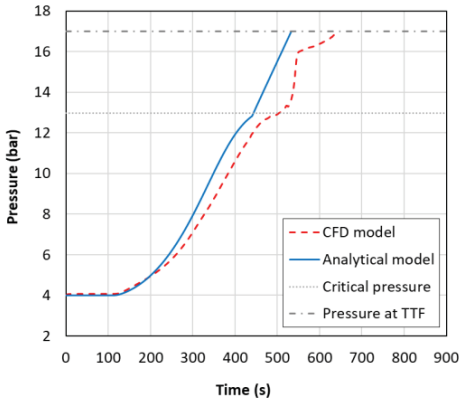

Figure 2: Comparison between the inner pressure obtained with the CFD model and the analytical model with an initial pressure of 4 bar until the TTF.

As shown in Figure 2, the pressurization rate of the tank obtained with the analytical approach is slightly higher than the one provided by the CFD model. Consequently, the time required to reach the critical pressure (444 s) is lower to the value provided by the CFD model.

The TTF of the tank is reached when the inner pressure is 17 bar. According to the analytical model, this happens after 532 s from the beginning of the simulation, while the CFD model foresees the rupture of the tank after 643 s.

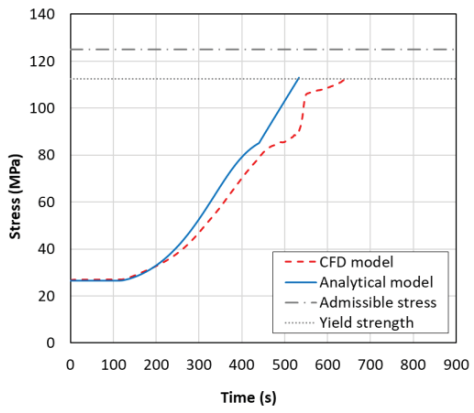

Figure 3: Comparison between the mechanical stress obtained with the CFD model and the analytical model with an initial pressure of 4 bar.

6. Discussion

The CFD model used in the present study is suitable to study cryogenic hydrogen storage tanks in external fire conditions. The CFD model is in good agreement with the analytical approach, despite the different dimension of their computational domain. In fact, in the CFD simulation the storage tank is schematized as a 2D object (Figure 1), while in the analytical model the vessel is reproduced in 3D. The information provided in this work in terms of pressurization rate and time to failure can support the development of the safety response in case of accident situations involving LH_2 vessels.

The major finding of the present study is the capability of the CFD model to simulate hydrogen behaviour in supercritical conditions. As expected, the results proves that this situation arises quickly (after 504 s) if is there are no active devices for pressure reduction. Although the simulation was successful, the pressure trend (Figure 2) shows some anomalies arising at the critical point, where the inner pressure suddenly increases. This result can be a consequence of the thermodynamic properties database, in particular the function implemented for the estimation of the specific heat of hydrogen. Values are selected from the NIST (2019) database and after the critical point, they are exclusively functions of the temperature and the pressure dependence is not considered. Figure 4 shows the corresponding curve for the gaseous phase. Due to the abrupt change of the specific heat, the vaporization of the liquid content is enhanced with the consequent pressure build-up. Further investigations are required to improve the function used to describe hydrogen properties, accounting also for the pressure dependence in supercritical conditions. In addition, the initial temperatures of the gas and liquid phases can be set equal to the BMW fire test (initial liquid temperature of 20 K and initial vapour temperature of 36 K) to assess how this influence the simulation results.

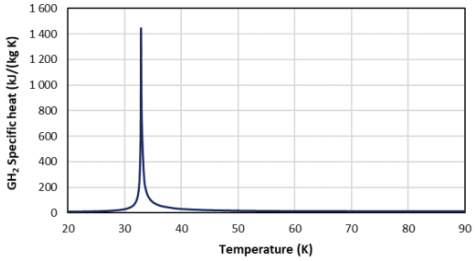

Figure 4: Specific heat of gaseous hydrogen (NIST, 2019).

7. Conclusions

The response of cryogenic hydrogen tank exposed to an external fire is investigated by means of a CFD analysis. The numerical model is used to reproduce the fire test conducted by the BMW Group on a LH_2 storage tank engulfed in a propane fire. The pressurization rate and the TTF of the vessel are conservatively estimated in the worst-case scenario, assuming the failure of the pressure relief device installed on the cryogenic equipment and the tank initially pressurized at 4 bar. It is demonstrated that the model can work both in subcritical and supercritical hydrogen conditions and conservatively estimates the TTF; thus, it is a valuable tool for safety assessment studies. However, the present approach needs to be validated with additional experimental data for supercritical conditions and further improvement is required.

Acknowledgment

This work was undertaken as part of the research project Safe Hydrogen Fuel Handling and Use for Efficient Implementation 2 (SHIFT-2), and the authors would like to acknowledge the

financial support of the Research Council of Norway under the ENERGIX programme (Grant No. 327009). This work was undertaken as part of the ELVHYS project No. 101101381 supported by the Clean Hydrogen Partnership and its members. UK participants in Horizon Europe Project ELVHYS are supported by UKRI gran numbers 10S063519 (University of Ulster) and 10070592 (Health and Safety Executive). Funded by the European Union Views and opinions expressed are however those of the author(s) only and do not necessarily reflect those of the European Union or Clean Hydrogen JU. Neither the European Union nor the granting authority can be held responsible for them.

References

Aziz, M., (2021). Liquid Hydrogen: A Review on Liquefaction, Storage, Transportation, and Safety. *Energies* 14, 5917.

Barron, R., Nellis, G., (2016). *Cryogenic Heat Transfer*. CRC Press.

BMW Group, (2007). BMW E68 http://www.bmwarchive.org/e-code/e68.html (accessed March 27, 2023).

Center for Chemical Process Safety, (1999). Guidelines for Consequence Analysis of Chemical Releases, American Institute of Chemical Engineers.

Crowl, D. A., Jo, Y., (2007). The hazards and risks of hydrogen. *Journal of Loss Prevention in the Process Industry* 20, 158-164.

Fesmire, J. E., (2017). Cylindrical Cryogenic Calorimeter Testing of Six Types of Multilayer Insulation Systems, *Cryogenics* 89.

Fesmire, J. E., Swagner, A. M., Jacobson, A., Notardonato, B., (2021). Energy Efficient Large-scale Storage of Liquid Hdyrogen, *2021 Cryogenic Engineering Conference and International Cryogenic Materials Conference (CEC-ICMC)*

Hebb, C. L., (2014). Out of this world.

Hwang, H. T., Varma, A., (2014). Hydrogen storage for fuel cell vehicles. *Current Opinion in Chemical Engineering* 5, 42-48.

Jeon, G., Park, J., Choi, S., (2021). Multiphase-thermal simulation on BOG/BOR estimation due to phase change in cryogenic liquid storage tanks. *Applied Thermal Engineering* 184, 116264.

Kamperveen, J. P., Sprijt, M. P. N., Reinders, J. E. A., (2016). Heat Load Resistance of Cryogenic Storage Tanks – Results of LNG Safety Program. TNO Report no. TNO 2016 R10352.

Köne, A. C., Büke T., (2010). Forecasting of CO_2 emissions from fuel combustion using trend analysis. *Renewable and Sustainable Energy Reviews* 14, 2906-2915.

National Institute of Standards and Technology (2019). NIST Chemistry WebBook, SRD 69.

Pehr, K., (1996). Experimental examinations on the worst-case behaviour of LH2/LNG tanks for passenger cars. *Proceeding of the 11th World Hydrogen Energy Conference*, 2169-2187.

Qiu, Y., Yang, H., Tong, L., Wang, L., (2021). Research Progress of Cryogenic Materials for Storage and Transportation of Liquid Hydrogen. *Metals* 11, 1101.

Rüdiger, H., (1992). Design characteristics and performance of a liquid hydrogen tanks system for motor cars. *Cryogenics* 32, 327-329.

Rybin, H., Krainz, G., Bartlok, G., Kratzer, E., (2005). Safety Demands for Automotive Hydrogen Storage Systems. *International Conference of Hydrogen Safety* 12.

Tarhan, C., Çil, M. A., (2021). A study on hydrogen, the clean energy of the future: Hydrogen storage methods. *Journal of Energy Storage* 40, 102676.

Ustolin, F., Iannaccone, T., Cozzani, V., Jafarzadeh, S., (2021). Time to Failure Estimation of Cryogenic Liquefied Tanks Exposed to a Fire. *e-proceedings of the 30th Safety and Reliability Conference.*

Ustolin, F., Paltrinieri, N., Landucci, G., (2020b). An innovative and comprehensive approach for the consequence analysis of liquid hydrogen vessel explosions. *Journal of Loss Prevention in the Process Industries* 68, 104323.

Ustolin, F., Salzano, E., Landucci, G., Paltrinieri, N., (2020a). Modelling liquid hydrogen bleves: A comparative assessment with hydrocarbon fuels, *Proceedings of the 30th European Safety and Reliability Conference and the 15th Probabilistic Safety Assessment and Management Conference.*

Ustolin, F., Scarponi G. E., Iannaccone, T., Cozzani, V., (2022b). Cryogenic Hydrogen Storage Tanks Exposed to Fires: a CFD Study. *Chemical Engineering Transactions* 90, 535-540.

Ustolin, F., Tolias, I.C., Giannissi, S. G., Venetsanos, A. G., Paltrinieri, N., (2022a). A CFD analysis of liquefied gas vessel explosions, *Process Safety and Environmental Protection* 159, 61-75.

Yin, L., Ju, Y., (2020). Review on the design and optimization of hydrogen liquefaction processes. *Front. Energy* 14, 530-544.